BJP British Journal of Pharmacology

DOI:10.1111/bph.12747
www.brjpharmacol.org

RESEARCH PAPER

Inhibition of COX-2-mediated eicosanoid production plays a major role in the anti-inflammatory effects of the endocannabinoid *N*-docosahexaenoylethanolamine (DHEA) in macrophages

Jocelijn Meijerink[1], Mieke Poland[1], Michiel G J Balvers[1], Pierluigi Plastina[1], Carolien Lute[1], Jvalini Dwarkasing[1], Klaske van Norren[1,2] and Renger F Witkamp[1]

[1]*Division of Human Nutrition, Wageningen University, Wageningen, The Netherlands, and*
[2]*Nutricia Advanced Medical Nutrition, Danone Research, Utrecht, The Netherlands*

Correspondence
Jocelijn Meijerink, Division of Human Nutrition, Wageningen University, P.O. Box 8129, 6700 EV Wageningen, The Netherlands. E-mail: jocelijn.meijerink@wur.nl

Received
7 August 2013
Revised
3 April 2014
Accepted
11 April 2014

BACKGROUND AND PURPOSE

N-docosahexaenoylethanolamine (DHEA) is the ethanolamine conjugate of the long-chain polyunsaturated *n*-3 fatty acid docosahexaenoic (DHA; 22: 6*n*-3). Its concentration in animal tissues and human plasma increases when diets rich in fish or krill oil are consumed. DHEA displays anti-inflammatory properties *in vitro* and was found to be released during an inflammatory response in mice. Here, we further examine possible targets involved in the immune-modulating effects of DHEA.

EXPERIMENTAL APPROACH

Antagonists for cannabinoid $(CB)_1$ and CB_2 receptors and $PPAR_\gamma$ were used to explore effects of DHEA on NO release by LPS-stimulated RAW264.7 cells. The possible involvement of CB_2 receptors was studied by comparing effects in LPS-stimulated peritoneal macrophages obtained from $CB_2^{-/-}$ and $CB_2^{+/+}$ mice. Effects on NF-κB activation were determined using a reporter cell line. To study DHEA effects on COX-2 and lipoxygenase activity, 21 different eicosanoids produced by LPS-stimulated RAW264.7 cells were quantified by LC-MS/MS. Finally, effects on mRNA expression profiles were analysed using gene arrays followed by Ingenuity® Pathways Analysis.

KEY RESULTS

CB_1 and CB_2 receptors or PPARs were not involved in the effects of DHEA on NO release. NF-κB and IFN-β, key elements of the myeloid differentiation primary response protein D88 (MyD88)-dependent and MyD88-independent pathways were not decreased. By contrast, DHEA significantly reduced levels of several COX-2-derived eicosanoids. Gene expression analysis provided support for an effect on COX–2-mediated pathways.

CONCLUSIONS AND IMPLICATIONS

Our findings suggest that the anti-inflammatory effects of DHEA in macrophages predominantly take place via inhibition of eicosanoids produced through COX-2.

LINKED ARTICLES

This article is part of a themed section on Cannabinoids 2013 published in volume 171 issue 6. To view the other articles in this section visit http://onlinelibrary.wiley.com/doi/10.1111/bph.2014.171.issue-6/issuetoc

Abbreviations

ACEA, arachidonyl-2′-chloroethylamide; AEA, *N*-arachidonoylethanolamine (anandamide); CB receptor, cannabinoid receptor; CT, cycle threshold; DHA, docosahexaenoic acid (22:6n-3); DHEA, *N*-docosahexaenoylethanolamine; EPA, eicosapentaenoic acid (20:5n-3); IPA, Ingenuity Pathways Analysis; IRAK, IL-1 receptor-associated kinase; LOX, lipoxygenase; MCP-1, monocyte chemotactic protein-1; MyD88, myeloid differentiation primary response protein D88; *n-3* LC-PUFA, (n-3) long-chain polyunsaturated fatty acid; NAEs, *N*-acyl ethanolamines; poly-IC, polyinosinic : polycytidylic acid; TLR, toll-like receptor; TRAF, receptor-associated factor; TRIF, TIR-domain-containing adapter-inducing interferon-b; TRVP1, transient receptor potential channel vanilloid subtype 1; XTT, colorimetric assay

Introduction

Long-chain omega-3 polyunsaturated fatty acids (*n-3* LC-PUFAs) including docosahexaenoic acid (DHA; 22: 6*n*-3) and eicosapentaenoic acid (EPA; 20: 5*n*-3) play important roles in normal tissue development, and their intake is associated with the prevention or amelioration of certain cardiovascular, neural and possibly other diseases (Russo, 2009; Calder, 2011). It is assumed that many of the health effects of *n-3* LC-PUFAs are related to modulation or resolution of an elevated inflammatory status, which often plays a primary or secondary role in these disorders (de Roos *et al.*, 2009; Calder, 2011; De Caterina, 2011). To explain their activity on inflammation different mechanisms are proposed, which are at least partly linked or act in parallel (Calder, 2011). Several studies found that DHA and EPA exert direct effects on receptors and key regulators of inflammatory processes (Chapkin *et al.*, 2009; Mullen *et al.*, 2010; Calder, 2011). One of the latest additions was the study of Oh *et al.* demonstrating that *n-3* LC-PUFAs can serve as natural ligands for the GPCR GPR120 (Oh *et al.*, 2010). Alternatively, indirect mechanisms can be involved that occur through incorporation of omega-3 fatty acids in cell phospholipid membranes at the expense of the highly abundant omega-6 fatty acid arachidonic acid. This causes a shift from the formation of arachidonic acid-derived PGs and LTs towards less potent pro-inflammatory pathways (Calder, 2011). In addition, resolvins and protectins can be formed from EPA and DHA, which are considered to be pivotal in the control of the duration and magnitude of inflammatory processes (Serhan and Chiang, 2008).

Recently, we found evidence for another mechanism by which DHA can modulate inflammation, namely via its *N*-acyl ethanolamine (NAE) metabolite *N*-docosahexaenoylethanolamine (DHEA) (Balvers *et al.*, 2010; Meijerink *et al.*, 2011). The formation of this endogenous metabolite is stimulated by increasing the proportion of omega-3 fatty acids in the diet (Berger *et al.*, 2001) and DHEA was found to display greater inhibitory effects than its parent DHA on the release of NO and monocyte chemotactic protein-1 (MCP-1) from activated macrophages (Meijerink *et al.*, 2011). DHEA belongs to the class of NAEs, of which several members have been shown to act as endogenous mediators. The best known representative of this group is the endocannabinoid anandamide (*N*-arachidonoylethanolamine anandamide, AEA) (Alexander and Kendall, 2007; Correa *et al.*, 2009; Pertwee *et al.*, 2010). The cannabinoid $(CB)_2$ receptor (Alexander *et al.*, 2013a) has been linked to the anti-inflammatory effects of anandamide and other endocannabinoids and is predominantly expressed by cells of the immune system (Bátkai *et al.*, 2007; Csóka *et al.*, 2009; Mukhopadhyay *et al.*, 2010; Basu and Dittel, 2011). At the same time it is clear that not all NAEs exclusively bind to CB_1 or CB_2 receptors, but often also (or instead) show affinity for GPR55, GPR18, GPR119, transient receptor potential channel vanilloid subtype 1 (TRPV1; see Alexander *et al.*, 2013b) or PPARs (Alexander and Kendall, 2007; Di Marzo *et al.*, 2007; Pertwee *et al.*, 2010; Maccarrone, 2013; for nomenclature see Alexander *et al.*, 2013c). In addition, anandamide acts on other key regulators of inflammation, including COX, and it can be metabolized by COX, lipoxygenase (LOX) or cytochrome P450 (CYP450) to products with activity on inflammatory processes (Rouzer and Marnett, 2011; for nomenclature see Alexander *et al.*, 2013d).

These diverse and apparently pleiotropic interactions between NAEs and inflammatory pathways prompted us to further explore the underlying mechanism(s) of action of DHEA in inflammation. Although DHEA has been shown to possess affinity for both CB_1 and CB_2 receptors (Sheskin *et al.*, 1997; Brown *et al.*, 2010), studies from our and other labs (Brown *et al.*, 2010) gave rise to questions about the involvement of the CB_2 receptor in at least some of its anti-inflammatory mechanisms. In the present paper, we first studied the contribution of the Toll-like receptor (TLR)3/TLR4 myeloid differentiation primary response protein D88 (MyD88)-(in)dependent signalling pathways, the potential involvement of NF-κB, and the possible effects on IFN-β. In addition, possible roles of CB_1 and CB_2 receptors and PPARγ in the DHEA-mediated effects were further examined. As the combined results were pointing towards an effect on eicosanoid formation we then undertook a series of LC-MS/MS

studies to measure eicosanoid profiles. To further explore our findings and to examine the possible relationships with other pathways, some gene array analyses followed by Ingenuity Pathways Analysis (IPA) were carried out in parallel.

Methods

Culture of RAW264.7 cells

Most of the experiments were performed with RAW264.7 macrophages obtained from the American Type Culture Collection (Teddington, UK). Cells were grown and maintained in DMEM supplemented with 10% FBS, penicillin and streptomycin (P/S) at 37°C in a 5% CO_2 humidified air atmosphere. Cells (2.5×10^5 cells mL^{-1}) were seeded into 96-well cell culture plates for nitrite, IL-6 and viability/cytotoxicity measurements [colorimetric assay (XTT)/LDH], or in 6-well plates (2.5×10^5 cells mL^{-1}) for IFN-β and PGE_2 (EIA), COX-2 Western blot and eicosanoid analysis, and incubated overnight.

Effects of DHEA, GP-1a, arachidonyl-2′-chloroethylamide (ACEA), rosiglitazone and antagonists on stimulated release of NO, cytokines/chemokines and PGE_2

Adherent cells were pre-incubated for 30 min with the test compound or vehicle in duplicate or triplicate. LPS concentrations and incubation times were based on the specific properties of the different inflammatory mediators and previously estimated responses in the cell line and in peritoneal macrophages. In the case of RAW264.7 cells, LPS or polyinosinic : polycytidylic acid (poly-IC) were added to a final concentration of 1 μg·mL^{-1} in combination with the test compound. Peritoneal macrophages were activated with 0.1 μg·mL^{-1} LPS to measure IL-6 release, and with 1 μg·mL^{-1} LPS to measure NO production. Ethanol was used as solvent for DHEA, GP-1a, ACEA, SR141716 and SR144528 and DMSO was used as a solvent for GW9662. In all cases final ethanol/DMSO concentration never exceeded 0.1% v v^{-1}. When studying effects of antagonists, these were added (0.01, 0.1, and 1 μM) 30 min before the ligands (5, 10 μM DHEA). After another 30 min of incubation LPS (1 μg·mL^{-1}) was added. Cells were then cultured for 48 h (24 h for peritoneal macrophages) after which NO or XTT/LDH were measured. Nitrite accumulated in the culture medium was measured as an indicator of NO production using the Griess method (Green *et al.*, 1982). Briefly, 100 μL of cell culture medium was mixed with 100 μL of Griess reagents and incubated at room temperature for 10 min. Absorbance was measured at 540 nm using a plate reader. IL-6 release in the culture medium was measured by ELISA after 16 h (peritoneal macrophages) or 24 h (RAW264.7 cells) of incubation. IFN-β was measured by ELISA following an incubation of 24 h. Production of PGE_2 (24 h) was initially measured using EIA only. Further analyses of eicosanoid patterns were performed using LC-MS/MS. The supernatant of treated RAW264.7 cells was used for both EIA and LC-MS/MS analyses. For eicosanoid analysis, medium aliquots were stored at –80°C until analysis in the presence of inhibitors of auto-oxidation as described previously (Balvers *et al.*, 2012b).

Assays for viability and cytotoxicity. Cell viability and potential cytotoxic effects of compounds added were determined by an XTT assay and by measuring LDH leakage. To measure XTT conversion the XTT Cell Proliferation Kit II from Roche Applied Science (Almere, The Netherlands) was used. Briefly, RAW264.7 cells were incubated for 48 h with the compounds and LPS. After incubation, supernatants were carefully removed (for LDH determination) and 100 μL of fresh medium supplemented with sodium 30-[1-(phenylaminocarbonyl)-3,4-tetrazolium]bis(4-methoxy-6-nitro) benzenesulfonic acid hydrate (XTT) (final concentration = 0.45 mM) and N-methyldibenzopyrazine methyl sulfate (1.25 mM), was added to the cells. After incubation at 37°C, the amount of formazan accumulated in the medium was measured at 450 nm on a plate reader (Multiskan Ascent, Thermo Labsystem, Breda, The Netherlands). Conditions were considered cytotoxic when formazan formation was >20% lower compared with untreated controls. LDH leakage was measured using a Cytotoxicity Detection Kit (Roche Applied Science, Almere, The Netherlands). LDH was measured in culture supernatants (100 μL), which were removed and mixed with enzyme reagents (diaphorase/NAD mixture, 250 μL) and dye solutions (iodotetrazolium chloride and sodium lactate, 11.25 mL). After 30 min of incubation at 25°C, the absorbance was measured at 492 nm.

Collection of peritoneal macrophages

To collect peritoneal macrophages, male C57Bl/6 ($CB_2^{+/+}$) and $CB_2^{-/-}$ (KO, knockout; B6.129P2-Cnr2tm1Dgen/J; The Jackson Laboratory, Bar Harbor, ME, USA) mice were used. For the studies described here, a total of five $CB_2^{-/-}$ and four $CB_2^{+/+}$ animals were used. Approval for this study had been obtained by the Local Committee for Care and Use of Laboratory Animals of Wageningen University. All studies involving animals are reported in accordance with the ARRIVE guidelines for reporting experiments involving animals (Kilkenny *et al.*, 2010; McGrath *et al.*, 2010). Both $CB_2^{-/-}$ and $CB_2^{+/+}$ mice had been bred for several generations in the experimental animal facilities of Wageningen University. They were housed two or three mice per cage in a temperature-controlled environment with a 12 h light–dark cycle (lights on between 06:00–18:00 h) and had free access to water and standard chow. Mice were first injected i.p. with a 4% Brewer Thioglycollate solution. Three days later, animals were killed and cells in the peritoneal cavity were collected by peritoneal lavage, using RPMI1640 medium containing P/S. The cell suspension was then centrifuged for 5 min at 280× *g* and 4°C and pellets were subsequently treated with erythrocyte lysis buffer (150 mM NH_4Cl, 10 mM $KHCO_3$, 0.1 mM EDTA) for 5–10 min on ice. Macrophages were collected and re-suspended in RPMI1640 containing 10% heat-inactivated (HI) FBS and P/S. Subsequently, they were counted and plated in a density of approximately 750.000 cells mL^{-1}. After 2 h, adhering macrophages were washed with PBS and cultured for 72 h in RPMI1640 medium (containing 10% FBS-HI and P/S) before stimulation. Q-PCR studies confirmed that the CB_2 gene was not expressed in the $CB_2^{-/-}$ peritoneal macrophages [cycle threshold (CT) values around 40] or in other tissues of the $CB_2^{-/-}$ mice, whereas the $CB_2^{+/+}$ peritoneal macrophages showed normal to high expression (CT values

around 25) of the CB_2 gene (CB_2 expression in peritoneal macrophages is shown in supplemental data).

NF-κB reporter assay

HEK293 cells were stably transfected with beta-galactosidase (LacZ) (InvivoGen, San Diego, CA, USA) and subsequently stably co-transfected with a luciferase reporter gene construct containing an eukaryotic promoter sequence with five NF-κB binding sites (pNiFty2-Luc, InvivoGen). For transfection, InvivoGen LyoVec was used according to the supplied protocol. For selection of LacZ transfected cells the antibiotic blasticidin (10 $\mu g \cdot mL^{-1}$) was added to the medium, while for cells co-transfected with pNiFty2-Luc, the addition of Zeocin (300 $\mu g \cdot mL^{-1}$) was also necessary. The antibiotics were added during selection and culturing of the cells, but were omitted during the subsequent experiments. All cells were cultured in DMEM with 4.5 $mg \cdot L^{-1}$ glucose and Glutamax, supplemented with 10% heat inactivated (HI) FBS and 1% P/S at 37°C and 5% CO_2.

To measure effects of DHEA on NF-κB-mediated luciferase activity, transfected HEK293 cells (6.5×10^5 cells mL^{-1}) were seeded into 96-well cell culture plates and incubated overnight. Cells were pre-incubated for 30 min with the test compound or vehicle in duplicate, and thereafter stimulated for 4 h with 50 ng TNF-α in the presence of the respective compound. Caffeic acid phenethyl ester (CAPE), a known inhibitor of NF-κB activation was used as a positive control. Experiments were performed in DMEM supplemented with 10% HI FCS and 1% P/S. As solvent ethanol was used (final solvent concentration never exceeded 0.1% v v^{-1}). For cell lysis and detection of TNF-α-induced NF-κB–luciferase activity, Britelite™ plus (Perkin Elmer, Groningen, The Netherlands) mixture was used in a 1:1 ratio, according to the manufacturer's protocol. Light emission was measured using an Ascent fluorescence meter (Thermo Labsystem).

COX-2 Western blotting

To determine effects of DHEA on COX-2 expression, adherent RAW264.7 macrophages were pre-incubated for 30 min with the test compound or vehicle in duplicate, after which LPS (1 $\mu g \cdot mL^{-1}$) was added in combination with the same test compound/vehicle. Ethanol was used as solvent for DHEA (final ethanol concentration never exceeding 0.1% v v^{-1}). Following 24 h of incubation, cells were lysed using lysis buffer (150 mM NaCl, 10 mM Tris-HCl pH 7.5, 5 mM EDTA, 1% Triton X-100) with a protease inhibitor cocktail (Roche) to determine COX-2 protein expression. Cell lysates were centrifuged at 16 000× *g* for 10 min at 4°C and the supernatants were then assessed for protein concentration. Fifteen micrograms of protein was separated by 10% mini-protean TGX precast gel (Bio-Rad, Veenendaal, The Netherlands) and transferred to a PVDF membrane using a Trans Blot Turbo Transfer System (Bio-Rad). The membrane was incubated with anti-COX-2 polyclonal antibody (dilution 1:1000) and anti-actin polyclonal antibody (dilution 1:2000) at 4°C overnight. The blot was washed and incubated with a secondary antibody (goat anti-rabbit HRP, dilution 1:5000) at room temperature for 1 h. Proteins were visualized by enhanced chemiluminescence (ECL) with a ChemiDoc^R image analyser (Bio-Rad).

Extraction and LC-MS/MS analysis of eicosanoids

To further investigate effects of DHEA on eicosanoid release patterns from LPS-stimulated RAW264.7 cells, we used LC-MS/MS applying a targeted lipidomic method as described previously (Balvers *et al.*, 2012b). This method allows the quantification of eicosanoids derived from several enzymatic pathways, covering COX-, LOX- and CYP450-derived metabolites. Briefly, 375 µL of cell culture medium was extracted with 1.5 mL methanol containing the appropriate internal standards, placed on ice for 30 min, and centrifuged for 5 min at 20 800× *g*. The supernatant was subsequently diluted with 6 mL MQ water containing 0.1% formic acid (FA) before solid phase extraction on HLB columns (Oasis; Waters, Etten-Leur, The Netherlands). After washing with 2 mL 20% methanol in MQ water with 0.1% FA, columns were eluted with 2 mL methanol and the eicosanoids were captured in glass tubes containing 20 µL of 500 µM butylated hydroxyethylene (BHT) and 10% glycerol in ethanol. After evaporation, under a gentle stream of nitrogen, the eicosanoids were reconstituted in 100 µL ethanol, and subsequently used for LC-MS/MS analysis. All eicosanoid analyses were performed on a UPLC coupled to a Xevo TQ-S tandem quadrupole mass spectrometer (Waters) as described previously (Balvers *et al.*, 2012b). In brief, 5 µL extract was injected on column, and all eicosanoids were separated on an Acquity C18 BEH UPLC column (2.1 × 100 mm, 1.7 µm) using a gradient elution with a stable flow at 600 $\mu L \cdot min^{-1}$. The MS was operated with electrospray in negative ion mode and eicosanoids were analysed in selective reaction mode. Cone voltage and collision energies were optimized for each compound individually. Peak identification and quantification was performed using MassLynx software version 4.1 (Waters, Etten-Leur, The Netherlands). Quality control samples were included in each analytical run to check the quality of the analysis and to correct for accuracy.

IPA

Upstream regulator analysis uses prior knowledge of published literature on effects between transcriptional regulators (any type of molecule, from transcription factor, to microRNA, kinase, compound or drug, that affects the expression of other molecules) and their target genes, which are stored in the Ingenuity Knowledge Base. The analysis predicts likely relevant transcriptional regulators by comparing the data sets of the studied compound with data sets in the Ingenuity Knowledge Base. The activation Z-score is a measure for the overlap in gene-expression profile induced by the studied compound with gene-expression profiles induced by upstream transcription regulators in the Ingenuity Knowledge Base (http://www.ingenuity.com/science/knowledge-base). The activation Z-score also takes the direction of the gene expression (up-regulated vs. down-regulated) into account. Positive values suggest overlapping profiles of sets of genes changed in a similar direction while negative values suggest opposite changes of sets of genes. Cut-off values for the activation Z-score are taken as 2 or –2. Statistical *P* values give significance of the observed overlap in gene-expression profiles.

For IPA, transcriptome data (for transcriptome analysis see Supporting Information) were used from three independent

experiments using LPS-stimulated RAW264.7 macrophages treated with 10 μM DHEA or vehicle. Experiments were conducted as described earlier.

Data analysis

All experiments in RAW264.7 macrophages were performed in duplicate, and those performed in the peritoneal macrophages were done as triplicate measures and repeated at least three times in independent experiments. Data from most experiments are expressed as a % of the LPS-treated controls (set at 100%). Data from the eicosanoid analyses are presented as absolute values. Data are presented as means with SEM (see legends to the figures). Statistical analyses were performed on the data as depicted in the figures, where differences between treatments and controls were evaluated by one-way ANOVA followed by *post hoc* test (in most cases Dunnett's *t*-test). To test statistical differences between $CB_2^{+/+}$ and $CB_2^{-/-}$ cells, variations were evaluated using repeated measures.

A P value < 0.05 was considered as statistically significant. P values were assigned at three different levels, namely $P < 0.05$, $P < 0.01$ and $P < 0.001$. For IPA activation, Z-scores are shown with P values < 0.01.

Materials

DHEA, rimonabant, 5-(4-chlorophenyl)-1-(2,4-dichlorophenyl)-4-methyl-N-1-piperidinyl-1H-pyrazole-3-carboxamide (SR141716), 5-(4-chloro-3-methylphenyl)-1-[(4-methylphenyl)methyl]-N-[(1S,2S,4R)-1,3,3-trimethylbicyclo[2.2.1]hept-2-yl]-1H-pyrazole-3-carboxamide (SR144528), PGE_2 EIA kits, Griess reagents including nitrite standard and analytical standards for eicosanoid analyses were bought from Cayman Chemical (Ann Arbor, MI, USA). GP-1a [N-(piperidin-1-yl)-1-(2,4-dichlorophenyl)-1,4-dihydro-6-methylindeno[1,2-c]pyrazole-3-carboxamide], reported to be a highly selective CB_2 agonist (Murineddu *et al.*, 2006) and ACEA were purchased from Tocris (Bristol, UK). LPS (*Escherichia coli* O111:B4), DHA, GW9662 (2-chloro-5-nitrobenzanilide), TMB (3,3′,5,5′-tetramethylbenzidine), BHT, BSA, ß-actin antibody, goat anti-rabbit HRP, rosiglitazone and CAPE (inhibitor of NF-κB (Natarajan *et al.*, 1996) were obtained from Sigma-Aldrich (Schnelldorf, Germany). DMEM, RPMI1640, FBS and P/S were purchased from Lonza (Verviers SPRL, Verviers, Belgium) and COX-2 antibody was acquired from Cell Signalling Technology (Danvers, MA, USA). Poly-IC (high molecular weight) a TLR3 ligand, specifically activating the MyD88-independent pathway, blasticidin S and zeocin were purchased from InvivoGen (San Diego, CA, USA) and PVDF membrane was acquired from Millipore (Amsterdam, The Netherlands). BCA protein assay and ECL were obtained from Pierce (Rockford, IL, USA). ELISA kits for IL-6 were bought from R&D Systems (Abingdon, UK). Brewer thioglycollate was acquired from BD Sciences (Franklin Lakes, NJ, USA) and ELISA kits for IFN-β were purchased from PBL Interferon Source (Piscataway, NJ, USA). Methanol was bought from Riedel-de-Haën (Steinheim, Germany) and ethanol from JT Baker (Deventer, The Netherlands). Nomenclature of drugs and receptors follows the BJP's *Concise Guide to Pharmacology* (Alexander *et al.*, 2013a,b,c,d).

Results

Cytotoxicity of test compounds

Results for cell viability/cytotoxicity (XTT and LDH) are shown in Supporting Information Table S1. DHEA alone or in combination with the antagonists rimonabant, SR144528, the combination of rimonabant and SR144528, or with GW 9662 did not affect cell viability in RAW264.7 macrophages at the concentrations tested. Data are shown for 5 and 10 μM DHEA, alone or in combination with 1 μM of each antagonist.

DHEA inhibits IL-6 production from mouse peritoneal macrophages and RAW264.7 cells

Effects of DHEA on the release of IL-6 was assessed for both LPS-stimulated C57Bl/6 mice peritoneal macrophages (Figure 1A) and RAW264.7 cells (Figure 1B). No IL-6 production could be measured in the absence of LPS-stimulation. In

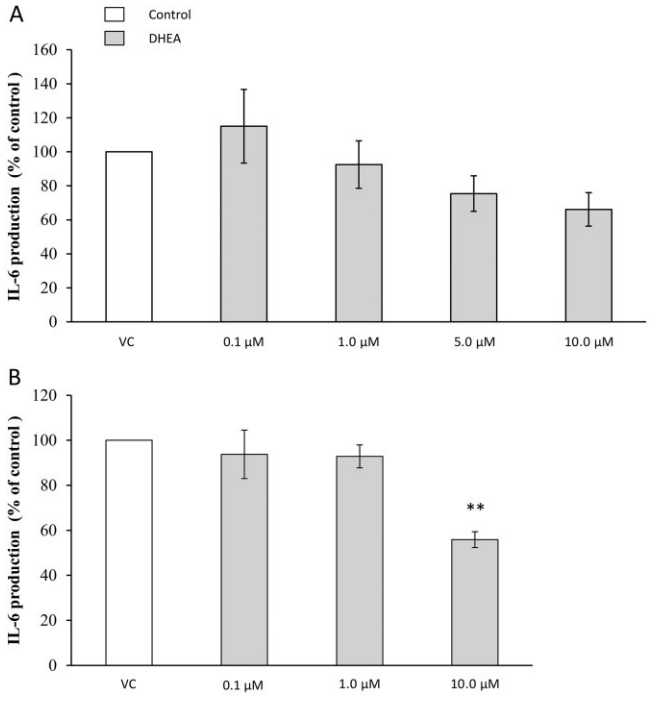

Figure 1

Inhibitory effect of DHEA on IL-6 release from LPS-stimulated C57Bl/6 mouse peritoneal macrophages (A) and RAW264.7 cells (B). Cells were pre-incubated with DHEA for 30 min before LPS stimulation and IL-6 was measured after 16 h (peritoneal macrophages) or 24 h (RAW264.7 cells) of incubation with DHEA or vehicle in the presence of LPS. Data are expressed as % of the IL-6 release with LPS and solvent only (=100%). Bars represent means ± SEM from four separate mice experiments (three measured in triplicate and one in duplicate; A), and four separate experiments with the RAW264.7 cell line (measurements in duplicate; B). Asterisks indicate significant difference from the control (one-way ANOVA, Dunnett's *t*-test; $^{**}P < 0.01$). IL-6 levels (ng·mL^{-1}) + SEM; for RAW264.7 cells, control 0; LPS 1 μg·mL^{-1} 31.4 + 2.6; DHEA 10 μM 17.5 + 1.9; for peritoneal macrophages, control 0; LPS 0.1 μg·mL^{-1} 3.1 + 1.6; DHEA 10 μM 1.7 + 0.7.

activated RAW264.7 cells, DHEA significantly reduced IL-6 production at 10 μM ($P < 0.01$). In C57Bl/6 mice peritoneal macrophages activated with LPS, a decreasing trend could be observed upon stimulation with increasing concentrations of DHEA. An EC_{50} value of 14.7 μM was determined for DHEA-induced NO reduction. The graph is presented in Supporting Information Figure S2.

Effects of DHEA on TLR/MyD88-dependent and -independent stimulation

To examine the involvement of TLR signalling pathways in the anti-inflammatory effects of DHEA, RAW264.7 cells were stimulated with the synthetic dsRNA analogue poly-IC, and results were compared with those obtained after LPS stimulation. Both LPS and poly-IC stimulation induced after 48 h a significant increase in NO levels. After poly-IC stimulation (MyD88-independent) DHEA reduced NO production (Figure 2) with a significant inhibition of approximately 35% at 10 μM DHEA; $n = 3$, $^*P < 0.05$ and $^{**}P < 0.01$. A concentration–dependent relationship was also obtained with LPS stimulation, achieving a higher maximal reduction at 10 μM DHEA (approximately 60%) compared with that using poly-IC.

DHEA does not inhibit NF-κB activation or IFN-β production

To investigate the possible interaction of DHEA with key inflammatory mediators involved in the MyD88-independent pathway and/or MyD88-dependent pathway, its effect on the activation of the transcriptional regulator NF-κB and on poly-IC stimulated IFN-β release were studied.

As shown in Figure 3, a concentration series of DHEA had no effect on the TNF-α induced activation of NF-κB measured both at 4 h (Figure 3A) and 24 h (not shown). Further screening at various time points (1.0, 2.5, 5.0, 16.0 and 48.0 h) also did not reveal any reduction of transcriptional activation of NF-κB in the luciferase reporter assay (data not shown). The positive control (CAPE) induced a significant reduction. DHEA at 1 μM and 10 μM did not have any reducing effect on IFN-β (a primary response gene product of the MyD88-independent pathway) protein levels in RAW264.7 cells stimulated with poly-IC (Figure 3B).

Effects of DHEA on NO *release appear to be independent from CB receptors and PPARγ*

The possible role of CB receptors and PPARγ in mediating DHEA-induced modulation of inflammatory mediators was explored. When comparing the effects of DHEA on NO production by peritoneal macrophages between $CB_2^{+/+}$ and $CB_2^{-/-}$ mice no significant differences were found between both groups (Figure 4). Furthermore, the highly selective CB_2 inverse agonist SR144528 (1 μM) did not significantly reverse the DHEA-induced NO reduction at 10 μM (Figure 5). In order to assess the possible involvement of the CB_1 receptor, the CB_1 inverse agonist SR141761 (rimonabant) was used. Both SR141761 (1 μM) alone and a combination of SR 141761 (1 μM) with the CB_2 inverse agonist SR144528 (1 μM) did not significantly reverse the DHEA-induced NO reduction at 10 μM (Figure 5). The CB_1 agonist ACEA (0.1, 1, 5, 10 μM) did induce a NO reduction of approximately 15%. However, this reduction was not concentration–dependent (Figure 5). Strikingly, the (reported) selective CB_2 agonist GP-1a was found to inhibit the production of NO (Figure 5) by LPS-stimulated RAW264.7 cells in a manner comparable with that of DHEA. However, additional experiments (using $CB_2^{-/-}$ peritoneal macrophages and SR144528) demonstrated that these GP-1a-

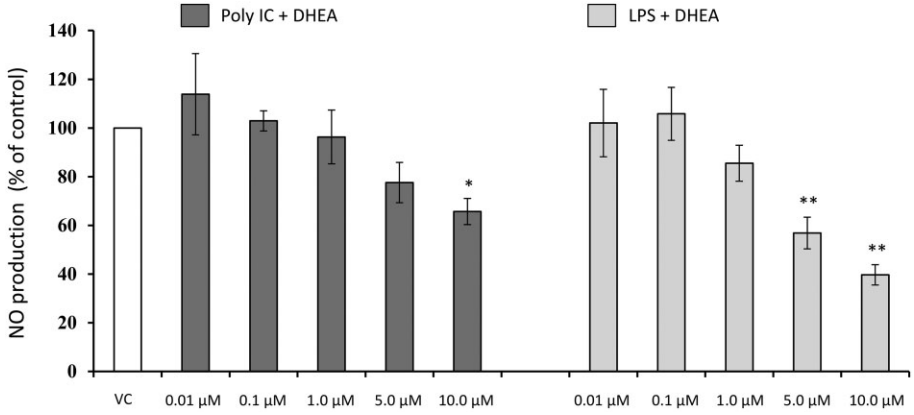

Figure 2

DHEA reduces NO release in both the MyD88-dependent and the MyD88-independent pathway. Dose–response graph showing poly-IC- and LPS-induced NO release modulated by DHEA in RAW264.7 mice macrophages. RAW264.7 macrophages were pre-incubated for 30 min with DHEA and stimulated for 48 h with either LPS or poly-IC (1 μg·mL^{-1}) in the presence of DHEA. Data are expressed as % of the NO release with LPS and solvent only (=100%). Bars represent means ± SEM from three separate experiments with duplicate measurements. Asterisks indicate significant difference from the control [one-way ANOVA, Dunnett's *t*-test (one-sided); $^*P < 0.05$ and $^{**}P < 0.01$]. [nitrite levels (μM) ± SEM: control 1.1 ± 0.7, poly-IC 1 μg·mL^{-1} 26.3 ± 5.6, DHEA 0.01 μM 29.8 ± 6.5, DHEA 0.1 μM 24.7 ± 3.9, DHEA 1 μM 24.9 ± 5.6, DHEA 5 μM 21.9 ± 4.5, DHEA 10 μM 18.6 ± 3.6 *; $n = 3$, $^*P < 0.05$ vs. poly IC alone]. [nitrite levels (μM) ± SEM: control 1.1 ± 0.3, LPS 1 μg·mL^{-1} 28.3 ± 2, DHEA 0.01 μM 29.8 ± 2.8, DHEA 0.1 μM 28.9 ± 1.9, DHEA 1 μM 23.2 ± 3, DHEA 5 μM 16.3 ± 3**, DHEA 10 μM 13.1 ± 2.1**; $n = 3$, $^{**}P < 0.01$ vs. LPS alone].

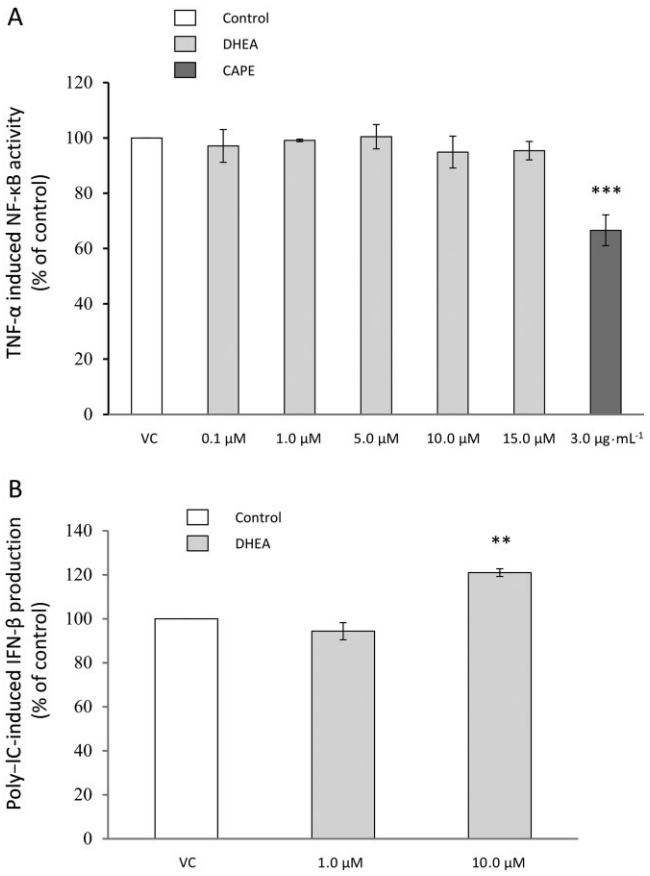

Figure 3

(A) Effect of DHEA on TNFα-induced NF-κB activity measured in a HEK293 NF-κB lacZ luciferase reporter assay containing a promoter sequence with five NF-κB binding sites. Cells were stimulated for 4 h with TNFα (50 ng·mL^{-1}) in the presence of different concentrations of DHEA (0.1, 1, 5, 10 and 15 μM). CAPE (3 μg·mL^{-1}), a synthetic NF-κB inhibitor was used as positive control. A 24 h time point gave similar results. (B) Effect of DHEA on IFN-β production of poly-IC stimulated RAW264.7 macrophages. Cells were stimulated for 24 h with poly-IC (1 μg·mL^{-1}) in the presence of 1 or 10 μM of DHEA. Experimental details are described in the Methods. Data are expressed as %, where TNFα (A) or poly-IC (B) stimulation (containing vehicle) was set at 100%. Data represent means ± SEM of three separate experiments (each done in duplicate). Asterisks indicate significant difference from the control (one-way ANOVA, Dunnett's *t*-test; $^{**}P < 0.01$, $^{***}P < 0.001$). IFN-β levels (ng·mL^{-1}) + SEM; control 0; poly-IC 1 μg·mL^{-1} 1.05 + 0.2; DHEA 10 μM 1.27 + 0.3.

induced inhibitory effects were not mediated by activation of CB_2 receptors (data not shown).

Figure 5 shows that the PPARγ antagonist GW9662 (1 μM) also did not reverse DHEA-induced effects on NO at 10 μM. The PPARγ agonist Rosiglitazone (1, 10 μM) itself did not affect NO production. Similar results were found with 0.1 or 0.01 μM of the antagonists rimonabant, SR144528, rimonabant and SR144528 combined and GW 9662 (Supporting Information Figure S3 shows results at 0.1 μM).

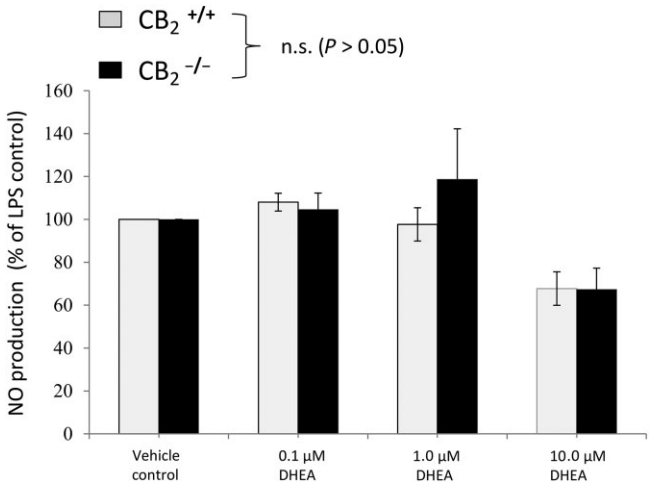

Figure 4

NO reduction induced by DHEA in LPS-stimulated peritoneal macrophages from $CB_2^{+/+}$ and $CB_2^{-/-}$ mice did not differ. Cells were pre-incubated for 30 min with each ligand (0.1, 1 or 10 μM) and NO levels were measured after 48 h stimulation with LPS (1 μg·mL^{-1}) in the presence of the respective ligand and concentration. Further details are described in the Methods. Data are expressed as a %, where LPS stimulation (containing vehicle) was set at 100%. Data represent means ± SEM of $n = 4$ $CB_2^{+/+}$ and $n = 5$ $CB_2^{-/-}$ mice (each done in triplicate). No significant difference (n.s.) was found between $CB_2^{+/+}$ and $CB_2^{-/-}$ (repeated measures). A significant overall treatment effect was found for DHEA.

DHEA inhibits PGE_2 production while only marginally affecting COX-2 expression

Next, it was studied whether DHEA interacts with targets downstream of NF-κB and IFN-β. For this, PGE_2 and other eicosanoids of the PLA_2- and COX-regulated pathways were selected. DHEA at a concentration of 1 μM was found to inhibit the release of PGE_2 (initially measured by EIA) from RAW264.7 cells by approximately 35%, while at 10 μM DHEA a 70% reduction was found (Figure 6A, left panel). By comparison, the parent compound DHA did not decrease, and even increased PGE_2 production when added to the cells (Figure 6A, right panel). Gene expression levels of COX-2 were not altered by 10 μM DHEA (Figure 6B). However, Western blot analysis showed that COX-2 protein levels were partly affected by DHEA stimulation (Figure 6C).

DHEA specifically reduces arachidonic acid-derived COX metabolites

To further characterize the effect of DHEA on the synthesis of eicosanoids, RAW264.7 macrophages were incubated with DHEA in the presence of LPS, and the eicosanoid concentrations in the medium were subsequently determined using a targeted lipidomics approach. This enabled the analysis of eicosanoids, which are derived from various enzymatic pathways, including COX, LOX and CYP metabolites. Only eicosanoids, which were altered by DHEA are depicted in Figure 7, with the complete data presented in the supplemental data (Supporting Information Table S2).

DHEA at 10 μM significantly reduced the medium levels of PGD_2, PGE_2, $PGF_{2\alpha}$, TXB_2, 8-iso-$PGF_{2\alpha}$ and 12-HHTrE (all

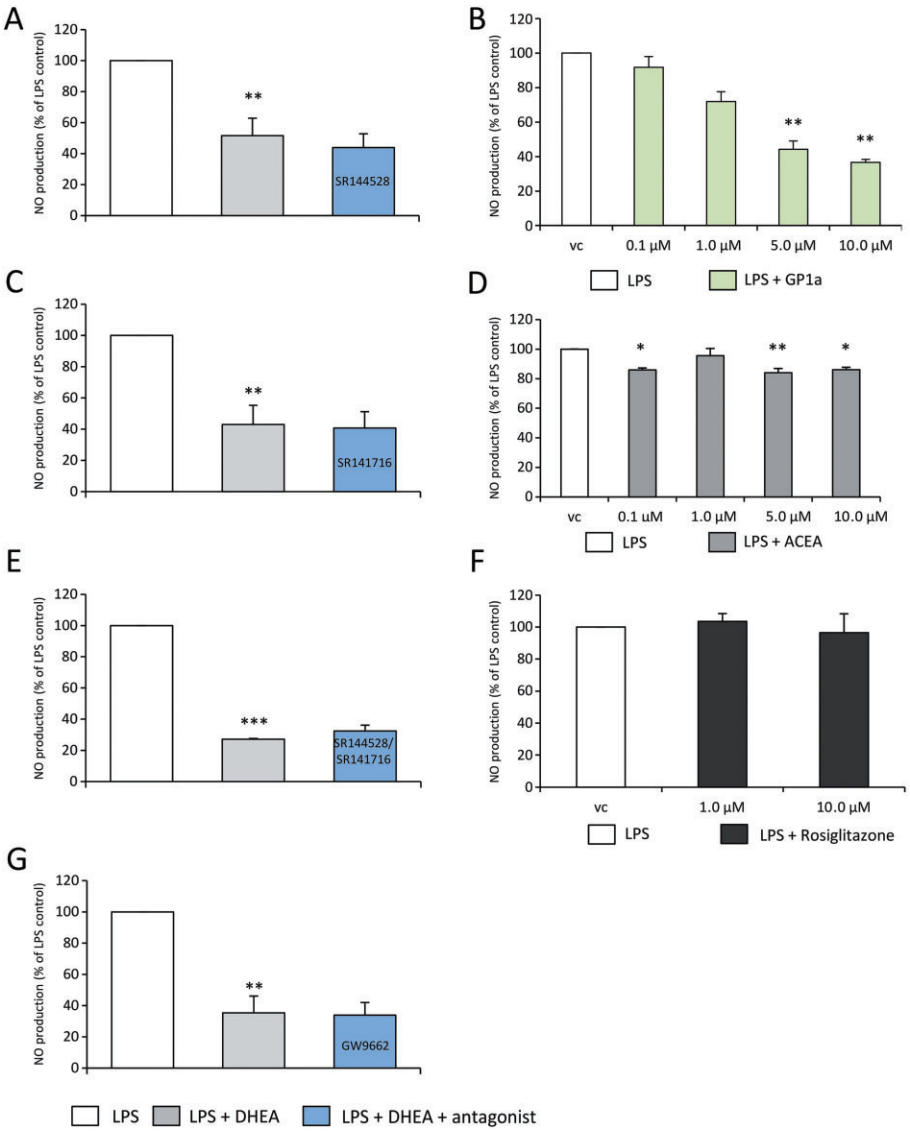

Figure 5

DHEA-induced reduction of NO production does not seem to involve the CB_1 or CB_2 receptors or PPARγ. NO reduction induced by DHEA in LPS-stimulated RAW264.7 macrophages was not significantly reversed by rimonabant, SR144528, a combination of rimonabant and SR144528, or GW9662 ($P > 0.05$ for all combinations). Cells were incubated for 30 min with 1 μM of the respective antagonist after which the regular pre-incubation with DHEA (10 μM) was started (see Methods for further details). NO levels were determined after 48 h LPS (1 $\mu g \cdot mL^{-1}$) stimulation in the presence of the respective antagonist and ligand. Data are expressed as %, where LPS stimulation (containing vehicle) was set at 100%. Data represent means ± SEM ($n = 3$–4 experiments; each done in duplicate). Statistical analysis was performed by one-way ANOVA, Dunnett's *t*-test, with $^*P < 0.05$ (with respect to LPS control), $^{**}P < 0.01$ (with respect to LPS control), $^{***}P < 0.001$ (with respect to LPS control). DHEA + antagonists (all combinations) were significantly different with respect to LPS control (not depicted in figure).

COX metabolites derived from arachidonic acid) to approximately 20–35%, and for TXB_2 to approximately 66% of the vehicle control values. PGD_2, $PGF_{2\alpha}$ and TXB_2 were also significantly reduced at 1 μM. A decreasing trend was observed for 15-deoxy-d-12,14-PGJ_2. The levels of the anti-inflammatory mediator 19,20-DiHDPA, a CYP450 metabolite derived from DHA, were increased approximately fourfold with 10 μM DHEA. No statistically significant effects were observed with 0.1 μM DHEA.

DHEA-induced inflammatory gene-expression profile supports inhibition of PGE_2 signalling pathway

Figure 8 shows the activation Z-scores of DHEA-induced gene-expression profiles in LPS-stimulated macrophages that displayed significant ($P < 0.01$) overlap with induced gene-expression profiles of upstream transcriptional regulators. Data were analysed using upstream regulator analysis with IPA. Highest overlap in the opposite direction for DHEA-

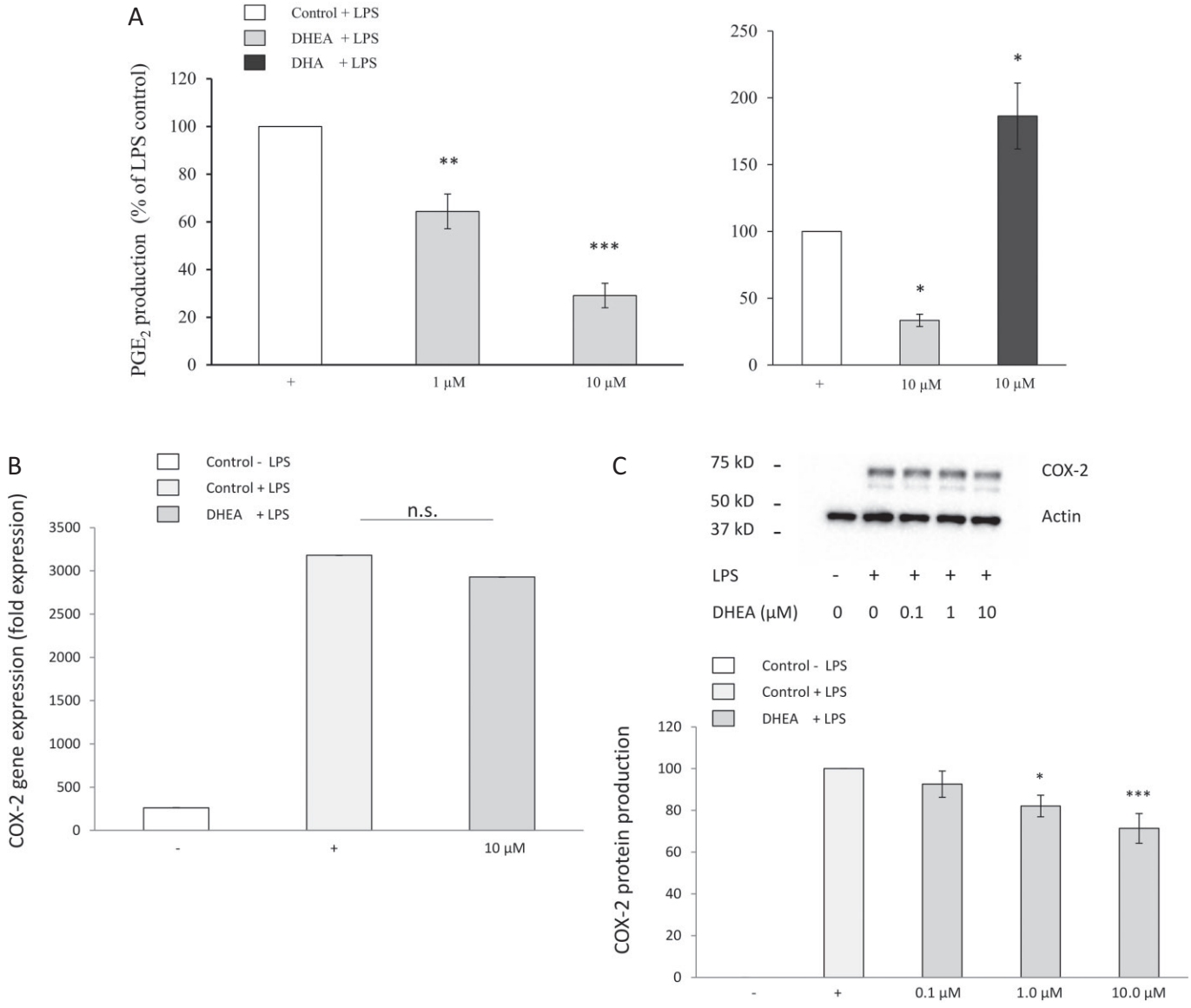

Figure 6

(A) DHEA reduced PGE_2 production in LPS-stimulated RAW264.7 macrophages. Cells were pre-incubated for 30 min with 1 or 10 μM DHEA and stimulated for 24 h with LPS (0.1 μg·mL^{-1}) in the presence of the respective ligand and concentration. Data represent means ± SEM of three separate experiments (each done in duplicate). The right figure shows the mean (± SEM) of another set of three separate experiments. Here, cells were stimulated with 1 μg·mL^{-1} LPS and treated with 10 μM DHA or 10 μM DHEA. All other conditions were similar as mentioned for the left figure. Experimental details are described in the Methods. Data are expressed as percentage, where LPS stimulation (containing vehicle) was set at 100%. Asterisks indicate significant difference from the control (one-way ANOVA, Dunnett's *t*-test; *$P < 0.05$, **$P < 0.01$ and ***$P < 0.001$). PGE_2 levels (pg·mL^{-1}) + SEM; for A, control 19.7 + 9.5; LPS 0.1 μg·mL^{-1} 204.1 + 81; DHEA 10 μM 49.6 + 10.1. (B) DHEA does not influence COX-2 at gene expression level. COX-2 expression was assessed using microarray analysis. Cells were pre-incubated for 30 min with 10 μM DHEA and stimulated for 24 h with LPS (0.1 μg·mL^{-1}) in the presence of DHEA. As control non–LPS-stimulated cells were used. Graph shows means ± SEM of three separate experiments (each performed in duplo), no significant effect was found (n.s.); *Q* value > 0.05. (C) DHEA partly influences COX-2 at the protein level. Upper, representative example of Western Blot analysis showing COX-2 protein in RAW264.7 macrophages after 24 h stimulation with 1 μg·mL^{-1} LPS with or without DHEA. Antibodies were used against COX-2 or the control actin. Lower panel shows densitometry of COX-2 protein expression, corrected for actin expression. Data show mean ± SEM of six independent experiments (each performed in duplicate). Asterisks indicate significant difference from the control (one-way ANOVA, Dunnett's *t*-test); *$P < 0.05$ ***$P < 0.001$.

induced inflammatory gene-expression profiles were found for the seven upstream transcriptional regulators TNF (–3.403), TLR3 (–3.077), IL-1 (–2.995), cholesterol (–2,811), LPS (–3.056) and PGE_2 (–2.508) and immunoglobulin (–2.346). All upstream regulators with activation Z-scores above a cut-off value of –2 or 2 are depicted in Figure 8 and complete data are presented in the Supporting Information. Three upstream transcriptional regulators showed overlap in gene expression-induced profiles in a direction similar to DHEA namely SB203580 (2.384), RPSA (2) and S100A6.

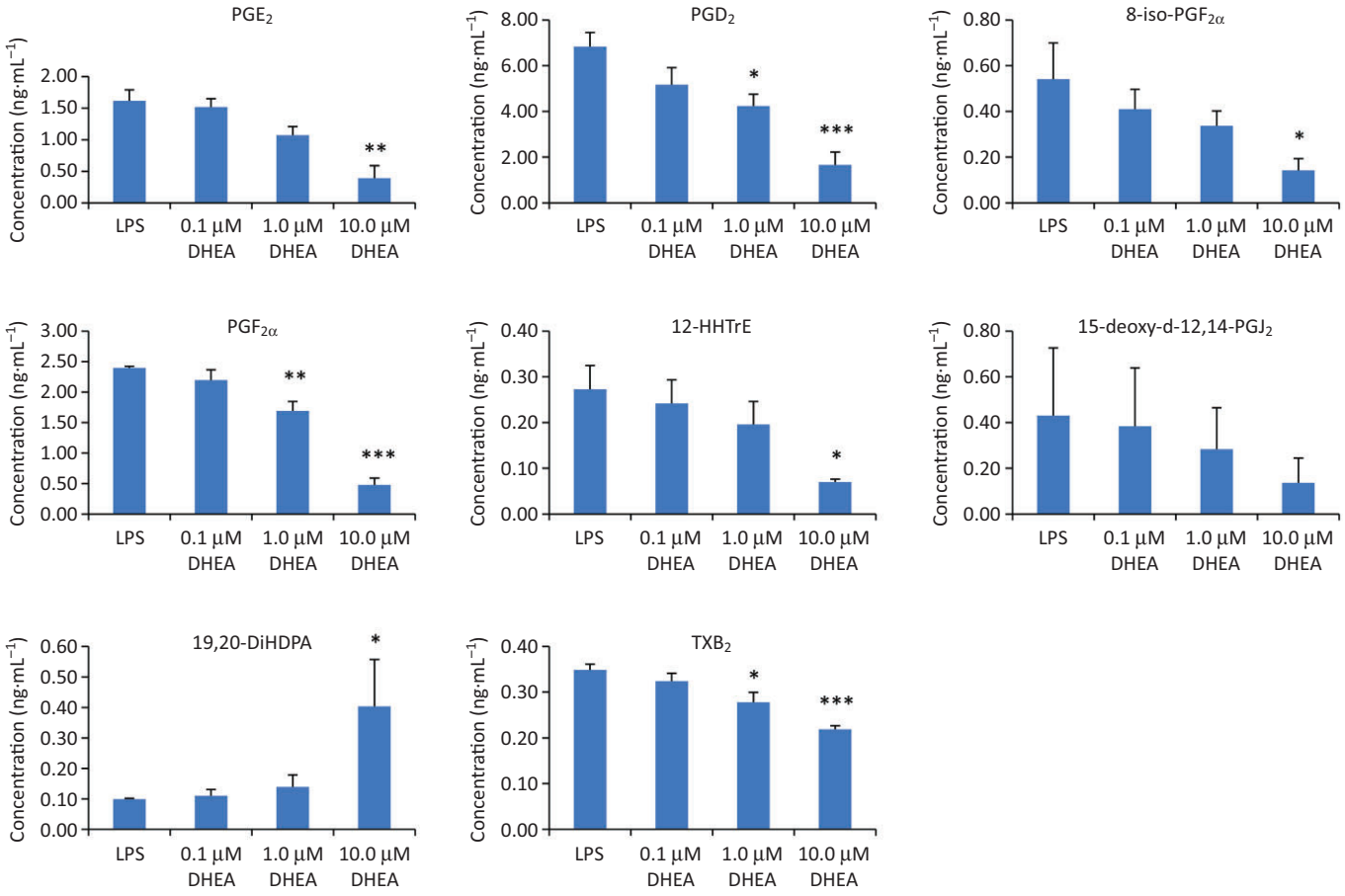

Figure 7

Effect of DHEA on eicosanoid synthesis of LPS-stimulated RAW264.7 macrophages. DHEA reduced medium levels of several COX-derived arachidonic acid eicosanoids, and increased the levels of 19,20-DiHDPA, a DHA metabolite, after LPS (1 μg.ml^{-1}) stimulation. Data represent means ± SEM of three independent experiments. Asterisks indicate significant difference from the control [one-way ANOVA, Dunnett's *t*-test (one-sided)]; **P* < 0.05 ***P* < 0.01 ****P* < 0.001.

Discussion

DHEA is an endogenous ethanolamine conjugate derived from the dietary important n-3 fatty acid DHA. Its presence has been demonstrated in several species and tissues, including bovine brain and retina (Sheskin *et al.*, 1997; Bisogno *et al.*, 1999), pig brain (Berger *et al.*, 2001), several tissues from rodents (Wood *et al.*, 2010; Balvers *et al.*, 2012b), and in human plasma (Balvers *et al.*, 2010; 2013). In a previous study, we demonstrated that DHEA can inhibit the release of NO and MCP-1 from LPS-activated macrophages (Meijerink *et al.*, 2011). This effect was at least partly mediated at a transcriptional level, as iNOS and MCP-1 mRNA levels were found to be reduced as well. In the present study, these findings were confirmed and the spectrum of anti-inflammatory activities of DHEA was found to include the modulation of IL-6 and eicosanoid release.

From its structural similarity to anandamide and other endocannabinoids it seemed obvious to start examining the question whether DHEA exerts its effects through CB_2 receptors. Indeed, DHEA has been reported to possess binding affinity to CB_2 (Brown *et al.*, 2010), which is in line with binding studies performed in our laboratory. Evidence for a role of CB_2 receptors in modulating different immune processes comes from a number of studies (Basu and Dittel, 2011). For example, Tschöp *et al.* showed that $CB_2^{-/-}$ mice were more sensitive to sepsis compared with WT controls (Tschöp *et al.*, 2009). In infected WT mice, the synthetic CB_2 ligand GP-1a, the same as used in our study, caused increased survival while reducing plasma IL-6 and bacteraemia. Apparently, effects of GP-1a were not tested in experimentally infected $CB_2^{-/-}$ mice in that study. In the present study, we did not observe a difference between activated peritoneal macrophages isolated from either $CB_2^{+/+}$ or $CB_2^{-/-}$ mice in NO reduction by DHEA. Evidence for the unlikelihood of a direct role of CB_2 receptors in the anti-inflammatory actions of DHEA was further supported by the observation that their effects could not be reversed by the CB_2 inverse agonist SR 144528. Interestingly, questions about the (full) role of CB_2 and/or selectivity of some (endo-) CBs or reported antagonists in modulating anti-inflammatory pathways also comes from other studies (Buckley, 2007; Kozela *et al.*, 2010). A certain

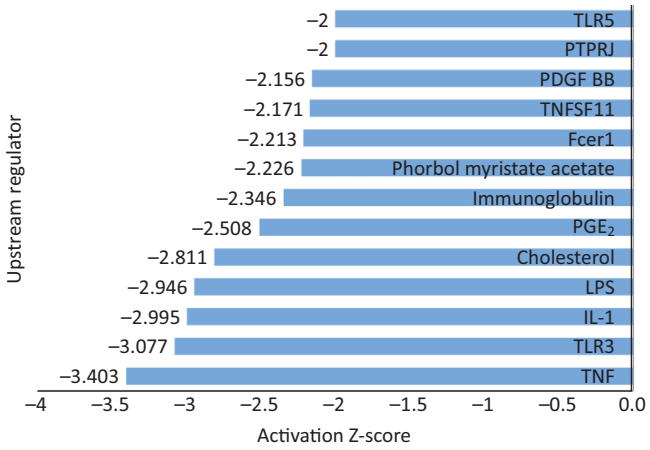

Figure 8

IPA showing activation Z-scores of upstream regulator mediators found to have highest overlapping opposite changes in gene-expression profiles compared with DHEA-induced gene-expression profiles. Activation Z-scores are shown for profiles significantly overlapping with $P < 0.01$ and cut off value of – 2.

degree of 'promiscuity' of presumed selective CB_2 ligands is also seen with other compounds, for example JWH-133 (reported potent, selective CB_2 agonist) and GW-405,833 (reported potent, selective partial CB_2 agonist), which were found to also interact with the GPR55 receptor (Anavi-Goffer *et al.*, 2012). Our results strongly suggest that the GP-1a induced inhibition of NO production is not mediated via CB_2 (data not shown) and raises some questions about the reported specificity of GP-1a. Although GP-1a has been documented to possess high agonist selectivity for CB_2 over CB_1 receptors (Murineddu *et al.*, 2006), this does not exclude the possiblity that the compound may also interact with molecular targets of inflammation besides CB_2 receptors.

Our results with the CB_1, CB_2 receptor and PPARγ antagonists, their combinations and the lack of a substantial effect of ACEA and rosiglitazone also do not suggest involvement of CB_1 or PPARγ receptors. These findings are in line with observations from other studies and models. For example, anti-proliferative effects mediated by DHEA in prostate cancer cell lines (Brown *et al.*, 2010) as well as DHEA-induced effects on neurite outgrowth and synaptogenesis in mice (Kim and Spector, 2013) were also found to be independent of CB receptors.

In the present study, it was found that DHEA not only inhibited NO release when cells were stimulated with LPS, but also, although to a lesser extent, after stimulation with poly-IC. Poly-IC is a synthetic RNA duplex specifically activating TLR3, thus simulating viral stimulation of the innate immune system. Activation of TLRs leads to the activation of different downstream signalling pathways resulting, amongst others, in the expression of pro-inflammatory cytokines and the induction of acquired immunity (Akira and Takeda, 2004; Kawai and Akira, 2010). Stimulation of TLR4 by LPS activates the so-called MyD88-dependent pathway. The latter involves the MyD88, TIR-domain-containing adapter-inducing interferon-b (TRIF), IL-1 receptor-associated kinase (IRAK) 4, IRAK1 and TNF receptor-associated factor (TRAF) 6 adaptor molecules. However, TLR4 stimulation also activates the so-called MyD88-independent pathway. The production of inflammatory cytokines via the MyD88-dependent pathway is mediated via activation of the early phase of NF-κB. The MyD88-independent pathway activates IFN-regulatory factor (IFN3) leading to the late phase of NF-κB activation and the production of IFN-β and IFN-inducible genes (Akira and Takeda, 2004; Kawai and Akira, 2010). Stimulation of TLR3 leads only to activation of the MyD88-independent signalling pathway. NO is produced during activation of both pathways. It has a pivotal function in inflammatory responses to pathogen intruders and is therefore tightly regulated. However, during chronic inflammatory conditions, harmful levels of NO are produced, which are thought to be involved in several diseases including insulin resistance and atherosclerosis (Detmers *et al.*, 2000; Charbonneau and Marette, 2010; Pilon *et al.*, 2010).

Our results demonstrate that DHEA reduces NO production both after activation of the MyD88-dependent (LPS) and the MyD88-independent (poly-IC) signalling cascades.

Our results provide no evidence for a direct interaction of DHEA with NF-κB activation. NF-κB is a central regulator of several inflammatory pathways. In our HEK293 NF-κB lacZ luciferase reporter assay DHEA did neither affect transcriptional activity of NF-κB itself, nor the activity of the IκB kinase complex. It also did not interfere with the TNF receptor-associated death domain/TRAF2 pathway as activated by TNF-α. In addition, IFN-β, a primary response gene product of the MyD88-independent pathway (Kawai and Akira, 2010), was not inhibited by DHEA after TLR3 stimulation with poly-IC at 24 h. As both the TNF-α-stimulated NF-κB lacZ luciferase reporter assay and the MyD88-independent pathway cannot activate TLR4 and the MyD88, TRIF, IRAK4, IRAK1 and TRAF6 adaptor molecules (Ruland, 2011), we cannot exclude the possibility that these adaptor molecules or the TLR4 itself are targeted by DHEA. Another plausible explanation, however, is that DHEA primarily targets mechanisms, which are located downstream of NF-κB or/and IFN-β and of which the most likely candidates are pathways regulated by cytosolic phospholipase A2, COX or LOX. Indeed, we obtained pronounced effects of DHEA on the production of PGE_2 and a number of other COX-derived eicosanoids. This suggests that DHEA inhibits the activity of these signalling pathways, likely by modulating a key inflammatory switch or an upstream regulator. The strongest inhibition was found for those metabolites (PGD_2, PGE_2, $PGF_{2\alpha}$, TXB_2, 8-iso-PGF2α and 12-HHTrE), which are formed through the action of COX-2 (Rouzer and Marnett, 2011). Upstream regulator analysis (IPA) of genes altered by DHEA, generating high activation Z-scores for the PGE_2 signalling pathway, independently provide further support for these findings. High activation Z-scores were also obtained for other pathways like TNF-(–3.403), TLR3-(–3.077) and LPS-(3.056). It should be noted that IPA scores alone are currently only suitable to generate or support hypotheses as results may be biased by the input of studies in the Ingenuity database. In addition, gene expression-induced profiles can be overlapping for partly overlapping or connected pathways. Microarray analysis showed that DHEA did not affect COX-2 gene expression after LPS stimulation. However, COX-2 protein levels were reduced to some extent

by DHEA, as stimulation with 10 μM resulted in 29% lower COX-2 protein levels compared with control. However, it seems unlikely that this reduction solely explains the large, up to almost 70%, inhibitory effects found on COX-2-derived PG levels. Therefore, we conclude that DHEA probably acts as a competitive or non-competitive inhibitor of COX-2. It is clear that substrate selectivity of COX-2 is not limited to arachidonic acid and that it also able to bind and metabolize other fatty acids and derivatives, including DHA and the endocannabinoids anandamide (AEA) and 2-arachidonoylglycerol. The latter generates PG ethanolamides (PG-EA) and PG glycerol esters respectively (Yu *et al.*, 1997; Kozak *et al.*, 2002; Rouzer and Marnett, 2011). Structure-activity studies showed that the terminal hydroxyl group of the ethanolamide moiety of AEA is crucial for the capability of COX-2 to utilize it as a substrate (Kozak *et al.*, 2003). Given the structural similarity of AEA and DHEA, carrying the same hydroxyl- and ethanolamide moiety and only differing in their C-atom chain length and number of double bounds, it is tempting to speculate that DHEA may act as substrate for COX-2. However, this would be subject to further investigation. Quite recently, novel DHEA-derived bioactive molecules formed through LOX enzymes have been identified (Yang *et al.*, 2011). In contrast to DHEA, parent DHA was found to increase levels of PGE_2 excreted by the RAW264.7 cells. This seems to be in line with results from human intervention studies from our laboratory showing that consumption of n-3 PUFA-rich shakes initially (during the first 6 h) induces pro-inflammatory gene-expression profiles in peripheral blood mononuclear cells (Bouwens *et al.*, 2010).

A principal effect of DHEA on eicosanoid production could also explain the results obtained with the other inflammatory mediators that were measured. It is conceivable that a reduction in PGE_2 production caused the reduction in NO release. Studies have shown that TLR3-induced iNOS expression in RAW264.7 cells is dependent on PGE_2 produced by COX-2 (Pindado *et al.*, 2007). In TLR4 stimulated glomerular mesangial cells, PGE_2 modulated NO production mainly occurred in a cAMP-dependent manner through the EP_4 receptor (Lin *et al.*, 2008). PGE_2 was also found to be capable of controlling the production of IL-6 via EP_4 in macrophages, in an animal model of rheumatoid arthritis (McCoy *et al.*, 2002), and in different cell types. For MCP-1 it was found that in the process of macrophage migration, activated PGE_2/EP_4 signalling up-regulates its expression (Tajima *et al.*, 2008). In previous studies, we demonstrated in mice that DHEA levels increased in different tissues after inducing an inflammatory response, an effect also seen with anandamide (Balvers *et al.*, 2012a,b). This could indicate that DHEA has a role as an endogenous anti-inflammatory mediator.

In conclusion, our data suggest that the anti-inflammatory effects of DHEA in macrophages are at least for a major part occurring through competitive or non-competitive inhibition of COX-2-derived eicosanoid production, most likely independently of CB_1 and CB_2 receptors or PPARγ. These effects are only to some extent associated with a reduction in COX-2 protein levels, which in turn was apparently not related to a reduced transcription of COX-2 mRNA. Further studies on the mechanism(s) involved and in particular their relevance for the *in vivo* situation (Calder, 2013) are warranted both from a pharmacological and a nutritional perspective.

Acknowledgements

We are grateful to Dr. T van Woudenbergh for her statistical advice and to Dr. M. Boekschoten for support and advice with the IPA and microarray analysis. The authors acknowledge Dr. I. Bobeldijk (TNO, Zeist, The Netherlands) and A. Verhoef, BSc (TNO Triskelion, Zeist, The Netherlands) for facilitating the oxylipin analyses.

Author contributions

J. M., M. P. and R. W. conceived and designed the experiments. M. P., M. B., P. P., C. L. and J. D. performed the experiments. J. M., M. P., M. B., P. P., J. D., K. N. analysed the data. M. B. and K. N. contributed reagents/materials/analysis tools. J. M. and R. W. wrote the paper.

Conflict of interest

The authors state no conflict of interest.

References

Akira S, Takeda K (2004). Toll-like receptor signalling. Nat Rev Immunol 4: 499–511.

Alexander SPH, Kendall DA (2007). The complications of promiscuity: endocannabinoid action and metabolism. Br J Pharmacol 152: 602–623.

Alexander SPH, Benson HE, Faccenda E, Pawson AJ, Sharman JL, Spedding M, Peters JA, Harmar AJ and CGTP Collaborators (2013a). The Concise Guide to PHARMACOLOGY 2013/14: G protein-coupled receptors. Br J Pharmacol 170: 1459–1581.

Alexander SPH, Benson HE, Faccenda E, Pawson AJ, Sharman JL, Spedding M, Peters JA, Harmar AJ and CGTP Collaborators (2013b). The Concise Guide to PHARMACOLOGY 2013/14: Ion channels. Br J Pharmacol 170: 1607–1651.

Alexander SPH, Benson HE, Faccenda E, Pawson AJ, Sharman JL, Spedding M, Peters JA, Harmar AJ and CGTP Collaborators (2013c). The Concise Guide to PHARMACOLOGY 2013/14: Nuclear hormone receptors. Br J Pharmacol 170: 1652–1675.

Alexander SPH, Benson HE, Faccenda E, Pawson AJ, Sharman JL, Spedding M, Peters JA, Harmar AJ and CGTP Collaborators (2013d). The Concise Guide to PHARMACOLOGY 2013/14: Enzymes. Br J Pharmacol 170: 1797–1867.

Anavi-Goffer S, Baillie G, Irving AJ, Gertsch J, Greig IR, Pertwee RG *et al.* (2012). Modulation of l-α-lysophosphatidylinositol/GPR55 mitogen-activated protein kinase (MAPK) signaling by cannabinoids. J Biol Chem 287: 91–104.

Bátkai S, Osei-Hyiaman D, Pan H, El-Assal O, Rajesh M, Mukhopadhyay P *et al.* (2007). Cannabinoid-2 receptor mediates protection against hepatic ischemia/reperfusion injury. FASEB J 21: 1788–1800.

Balvers MGJ, Verhoeckx KCM, Plastina P, Wortelboer HM, Meijerink J, Witkamp RF (2010). Docosahexaenoic acid and

eicosapentaenoic acid are converted by 3T3-L1 adipocytes to N-acyl ethanolamines with anti-inflammatory properties. Biochim Biophys Acta 1801: 1107–1114.

Balvers MGJ, Verhoeckx KCM, Meijerink J, Bijlsma S, Rubingh CM, Wortelboer HM *et al.* (2012a). Time-dependent effect of *in vivo* inflammation on eicosanoid and endocannabinoid levels in plasma, liver, ileum and adipose tissue in C57BL/6 mice fed a fish-oil diet. Int Immunopharmacol 13: 204–214.

Balvers MGJ, Wortelboer HM, Witkamp RF, Verhoeckx KCM (2013). Liquid chromatography–tandem mass spectrometry analysis of free and esterified fatty acid N-acyl ethanolamines in plasma and blood cells. Anal Biochem 434: 275–283.

Balvers MJ, Verhoeckx KM, Bijlsma S, Rubingh C, Meijerink J, Wortelboer H *et al.* (2012b). Fish oil and inflammatory status alter the n-3 to n-6 balance of the endocannabinoid and oxylipin metabolomes in mouse plasma and tissues. Metabolomics 8: 1130–1147.

Basu S, Dittel B (2011). Unraveling the complexities of cannabinoid receptor 2 (CB2) immune regulation in health and disease. Immunol Res 51: 26–38.

Berger A, Crozier G, Bisogno T, Cavaliere P, Innis S, Di Marzo V (2001). Anandamide and diet: inclusion of dietary arachidonate and docosahexaenoate leads to increased brain levels of the corresponding N-acylethanolamines in piglets. Proc Natl Acad Sci U S A 98: 6402–6406.

Bisogno T, Delton-Vandenbroucke I, Milone A, Lagarde M, Di Marzo V (1999). Biosynthesis and inactivation of N-arachidonoylethanolamine (anandamide) and N-docosahexaenoylethanolamine in bovine retina. Arch Biochem Biophys 370: 300–307.

Bouwens M, Grootte Bromhaar M, Jansen J, Müller M, Afman LA (2010). Postprandial dietary lipid-specific effects on human peripheral blood mononuclear cell gene expression profiles. Am J Clin Nutr 91: 208–217.

Brown I, Cascio MG, Wahle KW, Smoum R, Mechoulam R, Ross RA *et al.* (2010). Cannabinoid receptor-dependent and -independent anti-proliferative effects of omega-3 ethanolamides in androgen receptor-positive and -negative prostate cancer cell lines. Carcinogenesis 31: 1584–1591.

Buckley NE (2007). The peripheral cannabinoid receptor knockout mice: an update. Br J Pharmacol 153: 309–318.

Calder PC (2011). Fatty acids and inflammation: the cutting edge between food and pharma. Eur J Pharmacol 668 (Suppl. 1): S50–S58.

Calder PC (2013). Omega-3 polyunsaturated fatty acids and inflammatory processes: nutrition or pharmacology? Br J Clin Pharmacol 75: 645–662.

Chapkin RS, Kim W, Lupton JR, McMurray DN (2009). Dietary docosahexaenoic and eicosapentaenoic acid: emerging mediators of inflammation. Prostaglandins Leukot Essent Fatty Acids 81: 187–191.

Charbonneau A, Marette A (2010). Inducible nitric oxide synthase induction underlies lipid-induced hepatic insulin resistance in mice: potential role of tyrosine nitration of insulin signaling proteins. Diabetes 59: 861–871.

Correa FG, Mestre L, Docagne F, Borrell J, Guaza C (2009). The endocannabinoid anandamide from immunomodulation to neuroprotection. Implications for multiple sclerosis. Vitam Horm 81: 207–230.

Csóka B, Németh ZH, Mukhopadhyay P, Spolarics Z, Rajesh M, Federici S *et al.* (2009). CB_2 cannabinoid receptors contribute to bacterial invasion and mortality in polymicrobial sepsis. PLoS ONE 4: e6409.

De Caterina R (2011). n-3 fatty acids in cardiovascular disease. N Engl J Med 364: 2439–2450.

Detmers PA, Hernandez M, Mudgett J, Hassing H, Burton C, Mundt S *et al.* (2000). Deficiency in inducible nitric oxide synthase results in reduced atherosclerosis in apolipoprotein E-deficient mice. J Immunol 165: 3430–3435.

Di Marzo V, Bisogno T, De Petrocellis L (2007). Endocannabinoids and related compounds: walking back and forth between plant natural products and animal physiology. Chem Biol 14: 741–756.

Green LC, Wagner DA, Glogowski J (1982). Analysis of nitrate, nitrite, and [15N]nitrate in biological fluids. Anal Biochem 126: 131–138.

Kawai T, Akira S (2010). The role of pattern-recognition receptors in innate immunity: update on Toll-like receptors. Nat Immunol 11: 373–384.

Kilkenny C, Browne W, Cuthill IC, Emerson M, Altman DG (2010). Animal research: reporting *in vivo* experiments: the ARRIVE guidelines. Br J Pharmacol 160: 1577–1579.

Kim HY, Spector AA (2013). Synaptamide, endocannabinoid-like derivative of docosahexaenoic acid with cannabinoid-independent function. Prostaglandins Leukot Essent Fatty Acids 88: 121–125.

Kozak KR, Crews BC, Morrow JD, Wang LH, Ma YH, Weinander R (2002). 15-Lipoxygenase metabolism of 2-arachidonylglycerol. Generation of a peroxisome proliferator-activated receptor alpha agonist. J Biol Chem 277: 23278–23286.

Kozak KR, Prusakiewicz JJ, Rowlinson SW, Prudhomme DR, Marnett LJ (2003). Amino acid determinants in cyclooxygenase-2 oxygenation of the endocannabinoid anandamide. Biochemistry (Mosc) 42: 9041–9049.

Kozela E, Pietr M, Juknat A, Rimmerman N, Levy R, Vogel Z (2010). Cannabinoids Δ9-tetrahydrocannabinol and cannabidiol differentially inhibit the lipopolysaccharide-activated NF-κB and interferon-β/STAT proinflammatory pathways in BV-2 microglial cells. J Biol Chem 285: 1616–1626.

Lin K, Kools H, de Groot PJ, Gavai AK, Basnet RK, Cheng F *et al.* (2011). MADMAX – management and analysis database for multiple ~omics experiments. J Integr Bioinform 8: 160.

Lin YS, Hsieh M, Lee YJ, Liu KL, Lin TH (2008). AH23848 accelerates inducible nitric oxide synthase degradation through attenuation of cAMP signaling in glomerular mesangial cells. Nitric Oxide 18: 93–104.

Maccarrone M (2013). Endocannabinoid signaling in cancer: a rather complex puzzle. Trends Pharmacol Sci 34: 426–427.

McCoy JM, Wicks JR, Audoly LP (2002). The role of prostaglandin E2 receptors in the pathogenesis of rheumatoid arthritis. J Clin Invest 110: 651–658.

McGrath J, Drummond G, McLachlan E, Kilkenny C, Wainwright C (2010). Guidelines for reporting experiments involving animals: the ARRIVE guidelines. Br J Pharmacol 160: 1573–1576.

Meijerink J, Plastina P, Vincken J-P, Poland M, Attya M, Balvers M *et al.* (2011). The ethanolamide metabolite of DHA, docosahexaenoylethanolamine, shows immunomodulating effects in mouse peritoneal and RAW264.7 macrophages: evidence for a new link between fish oil and inflammation. Br J Nutr 105: 1798–1807.

Mukhopadhyay P, Rajesh M, Pan H, Patel V, Mukhopadhyay B, Batkai S *et al.* (2010). Cannabinoid-2 receptor limits inflammation, oxidative/nitrosative stress, and cell death in nephropathy. Free Radic Biol Med 48: 457–467.

Mullen A, Loscher CE, Roche HM (2010). Anti-inflammatory effects of EPA and DHA are dependent upon time and dose-response elements associated with LPS stimulation in THP-1-derived macrophages. J Nutr Biochem 21: 444–450.

Murineddu G, Lazzari P, Ruiu S, Sanna A, Loriga G, Manca I *et al.* (2006). Tricyclic pyrazoles. 4. Synthesis and biological evaluation of analogues of the robust and selective CB 2 cannabinoid ligand 1-(2′, 4′-dichlorophenyl)-6-methyl-N-piperidin-1-yl-1,4-dihydroindeno[1,2-c] pyrazole-3-carboxamide. J Med Chem 49: 7502–7512.

Natarajan K, Singh S, Burke TR Jr, Grunberger D, Aggarwal BB (1996). Caffeic acid phenethyl ester is a potent and specific inhibitor of activation of nuclear transcription factor NF-κB. Proc Natl Acad Sci U S A 93: 9090–9095.

Oh DY, Talukdar S, Bae EJ, Imamura T, Morinaga H, Fan W *et al.* (2010). GPR120 is an omega-3 fatty acid receptor mediating potent anti-inflammatory and insulin-sensitizing effects. Cell 142: 687–698.

Pertwee RG, Howlett AC, Abood ME, Alexander SPH, Di Marzo V, Elphick MR *et al.* (2010). International union of basic and clinical pharmacology. LXXIX. cannabinoid receptors and their ligands: beyond CB1 and CB2. Pharmacol Rev 62: 588–631.

Pilon G, Charbonneau A, White PJ, Dallaire P, Perreault M, Kapur S *et al.* (2010). Endotoxin mediated-INOS induction causes insulin resistance via ONOO- induced tyrosine nitration of IRS-1 in skeletal muscle. PLoS ONE 5: e15912.

Pindado J, Balsinde J, Balboa MA (2007). TLR3-dependent induction of nitric oxide synthase in RAW 264.7 macrophage-like cells via a cytosolic phospholipase A2/cyclooxygenase-2 pathway. J Immunol 179: 4821–4828.

de Roos B, Yiannis M, Ingeborg AB (2009). Long-chain n-3 polyunsaturated fatty acids: new insights into mechanisms relating to inflammation and coronary heart disease. Br J Pharmacol 158: 413–428.

Rouzer CA, Marnett LJ (2011). Endocannabinoid oxygenation by cyclooxygenases, lipoxygenases, and cytochromes P450: cross-talk between the eicosanoid and endocannabinoid signaling pathways. Chem Rev 111: 5899–5921.

Ruland J (2011). Return to homeostasis: downregulation of NF-kappaB responses. Nat Immunol 12: 709–714.

Russo GL (2009). Dietary n-6 and n-3 polyunsaturated fatty acids: from biochemistry to clinical implications in cardiovascular prevention. Biochem Pharmacol 77: 937–946.

Serhan CN, Chiang N (2008). Endogenous pro-resolving and anti-inflammatory lipid mediators: a new pharmacologic genus. Br J Pharmacol 153: S200–S215.

Sheskin T, Hanus L, Slager J, Vogel Z, Mechoulam R (1997). Structural requirements for binding of anandamide-type compounds to the brain cannabinoid receptor. J Med Chem 40: 659–667.

Tajima T, Murata T, Aritake K, Urade Y, Hirai H, Nakamura M *et al.* (2008). Lipopolysaccharide induces macrophage migration via prostaglandin D 2 and prostaglandin E2. J Pharmacol Exp Ther 326: 493–501.

Tschöp J, Kasten KR, Nogueiras R, Goetzman HS, Cave CM, England LG *et al.* (2009). The cannabinoid receptor 2 is critical for the host response to sepsis. J Immunol 183: 499–505.

Wood JT, Williams JS, Pandarinathan L, Janero DR, Lammi-Keefe CJ, Makriyannis A (2010). Dietary docosahexaenoic acid supplementation alters select physiological endocannabinoid-system metabolites in brain and plasma. J Lipid Res 51: 1416–1423.

Yang R, Fredman G, Krishnamoorthy S, Agrawal N, Irimia D, Piomelli D *et al.* (2011). Decoding functional metabolomics with docosahexaenoyl ethanolamide (DHEA) identifies novel bioactive signals. J Biol Chem 286: 31532–31541.

Yu M, Ives D, Ramesha CS (1997). Synthesis of prostaglandin E2 ethanolamide from anandamide by cyclooxygenase-2. J Biol Chem 272: 21181–21186.

Supporting information

Additional Supporting Information may be found in the online version of this article at the publisher's web-site:

http://dx.doi.org/10.1111/bph.12747

Figure S1 Q-PCR studies showing that the CB_2 gene was not expressed in the peritoneal macrophages from $CB_2^{-/-}$ mice (CT values around 40), whereas the $CB_2^{+/+}$ peritoneal macrophages showed normal to high expression (CT values around 25) of the CB_2 gene. $N = 3$ mice each.

Figure S2 EC-50 graph of DHEA-induced effects on NO. Macrophages (250.000 cells mL^{-1}) were pre-incubated for 30 min with a concentration series of DHEA prior to a 48 h LPS (1 $\mu g \cdot mL^{-1}$) stimulation, in the presence of the ligand. Data are expressed as percentage of the NO release with LPS and solvent only (=100%). Bars represent means ± SEM from four separate experiments with duplicate measurements.

Figure S3 Similar experiments as shown in Figure 5, but at 0.1 μM of antagonists. NO levels were determined after 48 h LPS (1 $\mu g \cdot mL^{-1}$) stimulation in the presence of the respective antagonist and ligand. Data are expressed as percentage, where LPS stimulation (containing vehicle) was set at 100%. Data represent means ± SEM ($n = 3$ experiments; each done in duplicate). Statistical analysis was performed by one-way ANOVA, Dunnett's *t*-test, with $^{**}P < 0.01$ (with respect to LPS control), $^{***}P < 0.001$ (with respect to LPS control) DHEA + antagonists (all combinations) were found significantly different with respect to LPS control (not depicted in figure).

Figure S4 Ingenuity pathways analysis (IPA) showing activation Z-scores of upstream regulator mediators found to have highest overlapping changes in similar direction in gene-expression profiles compared with DHEA-induced gene-expression profiles. Activation Z-scores are shown for profiles significantly overlapping with $P < 0.01$ and cut off value of 2.

Table S1 Viability/toxicity (XTT/LDH) data of RAW264.7 macrophages treated with DHEA in combination with different antagonist and with GP-1a, ACEA and rosiglitazone.

Table S2 All medium concentrations are in $ng \cdot mL^{-1}$. If no peak could be identified for a certain compound, than '<LOD' (limit of detection) was noted. If a certain compound concentration was below the limit of quantification (LOQ), then '<LOQ' was noted.